Crystal structure of cholestanyl caprylate and binary phase behavior with cholesteryl caprylate[1]

Gye Won Han and B. M. Craven

Department of Crystallography, University of Pittsburgh, Pittsburgh, PA 15260

Abstract The crystal structure of cholestanyl n-octanoate (caprylate) ($C_{35}H_{62}O_2$) is monoclinic with space group A2 and cell dimensions a = 10.103(7), b = 7.646(7), c = 87.63(7) Å, β = 90.51(6)°; Z = 8 [two molecules (A, B) in asymmetric unit], V = 6769 Å^3, Dc = 1.010 g cm^{-3}. Integrated X-ray intensities for 3798 reflections with $I > 2\sigma(I)$ were measured with a rotating anode diffractometer at room temperature. The structure was determined using direct methods. Block diagonal least squares refinement gave R = 0.111. Molecules A and B have almost fully extended conformations, but differ significantly in the rotation about the ester bond and in the C17 chains. The molecular packing in the crystal structure of cholestanyl caprylate consists of stacked bilayers each having d_{002} = 43.8 Å in thickness and within each bilayer, cholestanols pack with cholestanols and caprylate chains pack with caprylate chains. The crystal structure is very similar to that of cholesteryl myristate but is quite different from that of cholesteryl caprylate. The phase equilibria of the cholestanyl caprylate/cholesteryl caprylate binary system have been shown to involve limited mutual solubility of the two components and to have a eutectic point at 73% cholestanyl caprylate. The cholesteric mesophase is monotropic at all compositions except for a narrow range near the eutectic point where it is enantiotropic.—**Han, G. W., and B. M. Craven.** Crystal structure of cholestanyl caprylate and binary phase behavior with cholesteryl caprylate. *J. Lipid Res.* 1991. **32:** 1187–1194.

Supplementary key words cholestanyl ester • solid state substitution with cholesteryl ester

Cholestanyl caprylate (cholestanyl n-octanoate, **I**) ($C_{35}H_{62}O_2$, M = 514.88) is a fatty acid ester of cholestanol. Cholestanol is closely related to cholesterol, differing only by the absence of the C5–C6 double bond. Cholestanol and cholestanyl esters have been found in human plasma, erythrocytes, and bile (1), and in normal and atherosclerotic human aorta (2). They accumulate in pathological lipid deposits (xanthomas) in the brain and other tissues of patients with the rare inherited disease cerebrotendinous xanthomatosis (1).

Cholestanyl caprylate and the corresponding cholesterol ester (3) undergo similar phase transitions (4). Both form metastable mesophases obtained by undercooling the isotropic liquid.

76°C (m.p.)		106–108°C (m.p.)
crystal	→ isotropic liquid	crystal → isotropic liquid
↑	↓↑ 69°C	↑ ↓↑ 88°C
cholesteric mesophase		cholesteric mesophase
cholestanyl caprylate		***cholesteryl caprylate***

The crystal structure of the cholestanyl caprylate was first studied by Sawzik and Craven (5) using X-ray photographs. They found the crystal structure to be monoclinic with space group A2 at room temperature. Also, they reported that the molecular packing probably consists of bilayers similar to those in the crystal structure of cholesteryl myristate (6). However, more detailed information about the crystal structure, such as the atomic positional parameters and the molecular packing, was lacking. This investigation has provided the first detailed crystal structure determination of cholestanyl caprylate or of any fatty acid ester of cholestanol.

Although the corresponding cholesteryl ester (**II**), is chemically different only with respect to the presence of a C5=C6 ethylenic bond, we find that (**I**) and (**II**) have quite different crystal structures. Because of our interest in how cholestanyl and cholesteryl esters might substitute for each other in condensed lipid systems, we have undertaken a study of the binary phase behavior of the two caprylate esters.

[1]See NAPS document No. 04873 for 49 pages of supplementary material. Order from NAPS c/o Microfiche Publications, P.O. Box 3513, Grand Central Station, New York, NY 10163-3513. Remit in advance, in U.S. funds only, $16.45 for photocopies or $4.00 for microfiche. Outside the U.S. and Canada, add postage of $4.50 for the first 20 pages and $1.00 for each of 10 pages of material thereafter, or $1.50 for microfiche postage. There is a $15.00 invoicing charge for all orders not accompanied by payment; this includes P.O.#.

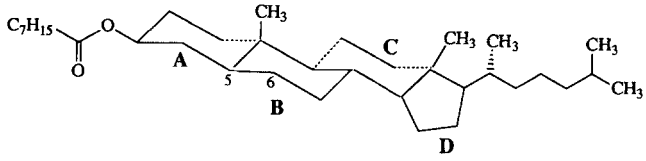

(I)

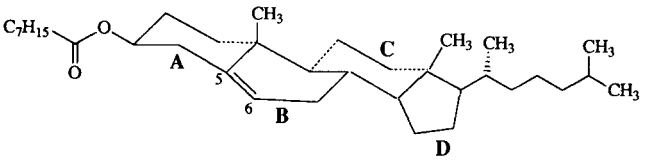

(II)

EXPERIMENTAL

Cholestanyl caprylate, obtained from Nu-Chek-Prep, Inc., Elysian, MN, was recrystallized slowly from a saturated solution in acetone–petroleum ether 50:50 at 273 K. Plate-like crystals formed, revealing broad {001} facets elongated along the crystallographic *b*-axis. Using a Mettler TA-4000 differential scanning calorimeter, we observed that the crystals melt at 77°C and on supercooling, undergo transition to the cholesteric phase at 68°C. In a subsequent study of the phase equilibria in the binary system cholesteryl caprylate/cholestanyl caprylate, the Mettler calorimeter was used in conjunction with a Leitz Wetzlar Laborlux 12 Pol polarized-light microscope equipped with a Leitz Heated Stage 350 and a temperature controller. Samples for differential scanning calorimetry were first heated above 125°C and then recooled to room temperature. This process was repeated several times to ensure intimate mixing of the phases. Most temperature scans were made at 5°C/min. The crystal-to-melt transition temperatures were determined from heating scans. Since the mesophase transition for some compositions was not easily observed during cooling, these transition temperatures were measured using the microscope. The solidus and liquidus curves in the phase diagram were constructed using peak temperature values for the transition endotherms in heating scans, while for solid solutions, an onset temperature (corresponding to the intersection of the extrapolated baseline and a line through the steepest part of the leading edge of the peak) and peak temperature were plotted. The samples used for calorimetry were also studied by powder X-ray diffraction at room temperature (CuKα radiation with Ni-filter; camera radius, 57.3 cm).

Single crystal X-ray data for cholestanyl caprylate were collected at room temperature (25°C) using an Enraf-Nonius CAD4 diffractometer and a rotating anode generator with graphite-monochromated CuKα radiation (λ = 1.5418 Å). The generator was operated at 4.3 KW. A crystal with dimensions (0.12 × 0.71 × 0.52 mm) was mounted with its b-axis close to the diffractometer ϕ-axis. Lattice parameters were determined by a least squares fit to the diffractometer setting angles for twelve reflections with $16 < 2\theta < 60°$C.

Crystal data[2] – $C_{35}H_{62}O_2$, M = 514.88, space group A2, a = 10.103(7), b = 7.646(7), c = 87.63(7) Å, β = 90.51(6)°, V = 6769 Å^3; Dc = 1.010 g cm^{-3}, Z = 8 (two molecules in asymmetric unit), μ = 4.570 cm^{-1}.

X-ray intensity data for cholestanyl caprylate were collected in two stages because the tungsten filament in the X-ray tube had to be replaced. The first measurements were thus done for 1509 reflections with $\theta < 45°$ at a $\omega/2\theta$ scanning rate of 1.6 min^{-1} in 2θ. After changing the filament, the data collection was continued until $\theta < 60°$ under the same scanning conditions. The two data sets were merged (R_{int} = 0.011), giving rise to the final intensity data set comprised of 5463 reflections of which 3798 reflections gave $I > 2\sigma(I)$. The variance in an integrated intensity was assumed to be $\sigma^2(I) = \sigma^2 + (0.02 \times I)^2$, where σ^2 was the variance due to counting statistics. No corrections were made for X-ray absorption.

The crystal structure was determined by direct methods with a random positional and orientational search for a tetracyclic ring taken from cholesteryl myristate (6) using the program MITHRIL (7). The E map revealed atomic positions of most atoms on the tetracyclic rings of molecules A and B and of some atoms in the caprylate chains of molecules. Structure factor calculations based on these atomic positional data assuming an overall B = 5 Å^2 and using scattering factors given by Cromer and Waber (8) resulted in an initial R = 0.35. The locations of the remaining atoms were then determined by reiterative Fourier methods.

The structure refinements were carried out by a block-diagonal least squares procedure, in which the function minimized was $\Sigma w\Delta^2$ where $\Delta = |Fobs| - |Fcal|$ and $w = 1/\sigma^2$ (Fobs). Damping factors of 0.5 and 0.2 were applied to the changes in atomic positional and thermal parameters, respectively. The 3798 reflections with $I > 2\sigma(I)$ were excluded in order to reduce computing time.

At R = 0.27, the positions for the hydrogen atoms were calculated assuming a standard bonding distance (1.0 Å) and angles from the carbon atom framework. Hydrogen atoms were taken into account in structure factor calculations by assuming their isotropic temperature factors to be the same as for the carbon atoms to which they are bonded. The hydrogen atom scattering factor was that

[2]It is to be noted that the present crystal data differ from those reported by Sawzik and Craven (4): a = 10.4(2), b = 7.7(1), c = 90.8(5) Å, β = 93(1)°, Vc = 7.26(21) × 10^3 Å^3. Since Sawzik and Craven's data were determined from Weissenberg photographs taken with Ni-filtered CuKα radiation, it is conjectured that the differences come from difficulties in indexing the high order reflections.

TABLE 1. Atomic positional and thermal parameters. The temperature factor has the form $\exp[-\Sigma_i\Sigma_j h_i h_j \beta_{ij}]$. E.s.d.s given in parentheses refer to the least significant digit. Top line, molecule A; bottom line, molecule B.

Atom	x/a (10^4)	y/b (10^4)	z/c (10^5)	$\beta 11$ (10^4)	$\beta 22$ (10^3)	$\beta 33$ (10^5)	$\beta 12$ (10^3)	$\beta 13$ (10^5)	$\beta 23$ (10^5)
O1	3413(06)	4188(13)	20552(07)	152(09)	56(03)	21(01)	107(15)	− 9(08)	24(18)
	3914(06)	9245(12)	19317(07)	145(09)	53(03)	21(01)	139(14)	89(08)	75(17)
O3	1843(06)	5429(10)	19122(06)	150(08)	31(02)	18(01)	28(12)	− 3(07)	− 13(13)
	5801(06)	10760(10)	19051(06)	124(08)	33(02)	17(01)	16(11)	20(07)	8(13)
C1	2796(10)	3153(15)	15455(10)	201(16)	20(03)	18(02)	56(18)	59(13)	6(19)
	6730(10)	11705(14)	14977(10)	195(16)	19(03)	18(02)	− 8(17)	21(13)	− 7(18)
C2	2259(09)	3405(15)	17042(10)	163(14)	19(03)	21(02)	42(17)	36(13)	25(20)
	6493(10)	11946(14)	16693(11)	184(16)	19(03)	21(02)	5(17)	4(14)	8(20)
C3	2542(08)	5108(15)	17676(10)	91(10)	29(03)	18(02)	47(16)	14(10)	12(20)
	5803(09)	10457(15)	17407(10)	146(13)	24(03)	16(02)	6(17)	− 17(11)	− 16(19)
C4	2219(09)	6617(15)	16633(10)	136(13)	27(03)	17(02)	− 26(17)	− 14(12)	− 21(19)
	6527(09)	8753(15)	17065(10)	123(12)	28(03)	19(02)	23(17)	− 11(12)	− 47(20)
C5	2863(08)	6338(14)	15083(10)	98(11)	22(03)	18(02)	− 13(15)	3(11)	− 11(18)
	6744(08)	8486(13)	15366(09)	96(11)	15(02)	18(02)	20(13)	0(11)	− 23(17)
C6	2649(09)	7926(14)	14063(10)	164(14)	20(03)	18(02)	− 23(17)	6(12)	− 25(19)
	7341(09)	6741(13)	15036(10)	146(13)	16(02)	21(02)	− 1(15)	46(12)	− 27(18)
C7	3368(08)	7755(14)	12544(10)	107(12)	21(03)	23(02)	− 1(15)	− 19(12)	28(19)
	7463(08)	6418(13)	13360(10)	111(12)	16(02)	25(02)	− 12(14)	− 10(12)	49(19)
C8	3130(08)	5985(13)	11765(09)	80(10)	19(02)	19(02)	16(13)	− 12(10)	− 22(17)
	8121(08)	7961(12)	12475(10)	83(10)	12(02)	24(02)	24(12)	− 17(11)	− 20(17)
C9	3277(08)	4452(12)	12873(09)	105(10)	9(02)	19(02)	− 8(12)	− 17(10)	9(16)
	7492(08)	9701(11)	12904(09)	129(11)	8(02)	18(02)	0(13)	− 13(11)	− 28(15)
C10	2463(08)	4625(12)	14371(10)	127(11)	10(02)	19(02)	16(13)	50(11)	− 4(16)
	7482(08)	10011(12)	14650(09)	145(12)	14(02)	14(01)	− 38(14)	13(10)	− 11(16)
C11	3121(10)	2701(14)	12010(10)	201(16)	18(03)	17(02)	0(17)	12(13)	11(18)
	8101(10)	11191(14)	11932(11)	177(15)	15(02)	23(02)	− 1(16)	30(13)	30(19)
C12	3947(10)	2543(15)	10585(11)	205(16)	24(03)	20(02)	24(19)	49(14)	− 44(21)
	8098(09)	10835(14)	10219(10)	182(15)	20(03)	20(02)	− 17(17)	28(13)	− 13(20)
C13	3681(08)	4040(13)	9468(10)	145(13)	14(02)	19(02)	26(15)	27(12)	16(17)
	8781(08)	9095(13)	9849(09)	126(12)	19(02)	16(02)	− 22(15)	− 17(11)	− 31(18)
C14	3972(07)	5740(12)	10349(09)	80(10)	13(02)	20(02)	24(13)	17(10)	33(17)
	8052(08)	7681(12)	10740(10)	132(12)	11(02)	19(02)	− 3(14)	8(11)	17(16)
C15	4016(09)	7137(15)	9183(10)	124(13)	25(03)	22(02)	7(16)	21(12)	18(21)
	8562(10)	5969(14)	10052(11)	192(15)	17(03)	23(02)	9(17)	− 26(14)	6(20)
C16	4616(09)	6271(15)	7746(12)	133(13)	23(03)	29(02)	− 19(17)	10(14)	− 52(22)
	8755(10)	6389(16)	8355(10)	185(16)	29(03)	19(02)	− 14(19)	− 5(13)	41(21)
C17	4730(08)	4269(16)	8120(09)	132(12)	31(03)	14(01)	18(17)	17(11)	30(20)
	8614(09)	8395(15)	8154(10)	144(13)	25(03)	19(02)	− 38(17)	− 24(12)	38(20)
C18	2280(08)	3989(17)	8772(11)	87(11)	39(04)	25(02)	− 15(18)	− 25(12)	− 27(24)
	10291(08)	9177(17)	10236(10)	74(10)	45(04)	18(02)	26(18)	3(10)	− 34(23)
C19	940(08)	4527(16)	13930(10)	57(09)	37(03)	24(02)	− 26(16)	− 8(11)	− 12(23)
	8968(08)	10139(16)	15251(10)	96(11)	35(03)	18(02)	73(17)	− 29(10)	− 2(21)
C20	4608(09)	3090(18)	6714(10)	176(15)	40(04)	15(02)	34(21)	57(13)	− 21(22)
	9462(10)	9171(21)	6863(10)	187(16)	62(05)	14(02)	35(26)	5(13)	28(27)
C21	4605(12)	1126(16)	7009(12)	312(22)	18(03)	31(02)	23(22)	53(19)	7(24)
	9396(12)	11241(17)	6692(12)	304(22)	27(03)	25(02)	− 10(24)	27(18)	− 50(24)
C22	5778(10)	3589(19)	5673(12)	204(17)	39(04)	25(02)	16(23)	51(15)	− 50(25)
	9015(15)	8260(25)	5377(13)	447(30)	56(05)	22(02)	47(38)	− 9(21)	44(33)
C23	5800(17)	2829(22)	4077(15)	508(36)	39(05)	36(03)	29(38)	− 38(26)	− 81(36)
	10041(19)	8515(31)	4034(14)	687(45)	81(08)	22(03)	129(57)	130(28)	132(41)
C24	7003(00)	3356(00)	3162(00)	339(28)	140(01)	41(03)	3(55)	260(26)	− 80(62)
	11355(22)	7660(44)	4135(23)	552(46)	135(16)	67(06)	− 490(76)	39(40)	117(82)
C25	7117(00)	2637(00)	1555(00)	1119(91)	207(24)	70(07)	198(142)	694(69)	131(126)
	12200(00)	7800(00)	2800(00)	521(46)	312(32)	57(05)	− 265(102)	65(38)	830(120)
C26	8556(00)	3209(00)	1183(00)	595(54)	181(20)	119(09)	52(105)	547(63)	− 250(140)
	13729(00)	7835(00)	3056(00)	564(50)	199(22)	89(07)	806(103)	328(52)	147(129)
C27	7151(00)	646(00)	1535(00)	1128(122)	470(72)	171(17)	− 753(272)	815(128)	− 1511(338)
	11679(00)	9298(00)	1914(00)	806(82)	64(90)	119(11)	572(240)	630(81)	1506(301)
C28	2394(08)	4948(15)	20466(10)	109(11)	30(03)	16(02)	7(16)	− 15(10)	− 6(19)
	4781(08)	10115(13)	19846(09)	108(11)	21(03)	17(02)	10(15)	6(10)	− 5(18)
C29	1487(09)	5476(17)	21742(10)	135(13)	37(03)	16(02)	10(19)	20(11)	31(22)
	4961(08)	10524(14)	21504(09)	135(12)	21(03)	14(01)	21(15)	− 3(10)	− 6(17)
C30	1946(08)	4844(15)	23292(09)	114(11)	31(03)	15(01)	34(17)	30(11)	− 31(19)
	3953(07)	9867(15)	22578(09)	82(10)	35(03)	16(02)	− 5(16)	30(10)	14(19)
C31	987(09)	5366(15)	24523(10)	159(13)	26(03)	19(02)	− 15(18)	− 12(12)	− 7(21)
	4222(09)	10387(15)	24224(10)	127(12)	24(03)	20(02)	7(17)	− 16(11)	4(20)
C32	1403(08)	4822(16)	26122(10)	118(12)	35(03)	19(02)	32(18)	− 11(11)	− 17(21)
	3284(09)	9807(16)	25402(10)	142(13)	32(03)	20(02)	6(19)	31(12)	18(22)
C33	407(08)	5349(15)	27340(10)	123(12)	27(03)	21(02)	− 17(17)	20(12)	− 11(21)
	3595(08)	10327(16)	26996(10)	87(11)	31(03)	20(02)	− 11(16)	− 10(11)	0(21)
C34	738(10)	4886(18)	29000(11)	191(16)	41(04)	21(02)	− 40(22)	− 82(14)	74(25)
	2641(10)	9802(18)	28182(11)	166(15)	43(04)	22(02)	− 29(22)	43(14)	23(26)
C35	− 261(10)	5485(22)	30162(11)	190(16)	71(06)	16(02)	55(28)	87(14)	− 31(29)
	3021(11)	10408(23)	29820(11)	247(20)	59(05)	17(02)	− 41(29)	10(15)	7(29)

of Stewart, Davidson, and Simpson (9). Anisotropic thermal parameters were introduced for the carbon and oxygen atoms at R = 0.14. An electron density map obtained at R = 0.112 showed an abnormally diffuse distribution at the terminal isopropyl group which consists of atoms C25, C26, and C27 of molecules A and B, and C24 of molecule A. Consequently, the calculated bond distances and angles were less satisfactory in this region. In each of these regions, positional parameters were revised by inspection of the electron density map displayed by computer graphics using the program FRODO (10). In the subsequent least squares refinement process, we fixed the positions of fitted atoms and included only their anisotropic thermal parameters as variables. In the end, a final R value of 0.111 was attained with R_w = 0.116 and goodness-of-fit S = 2.775.[3] Final atomic parameters are listed in **Table 1.**

DISCUSSION

Molecular structure

The average bond distances and angles for the crystallographically independent molecules A and B (***Fig. 1***) are almost identical, within experimental error, with those found in cholesteryl myristate (6) and other related structures (11–14), except for those for the cholestanyl tails. The estimated standard deviation is in the range 0.011–0.032 Å in bond lengths and 0.7–1.8° in bond angles. In the tetracyclic rings, the C–C distances and bond angles range from 1.46 to 1.60 Å and 100.0° to 120.0°, respectively.

The tetracyclic systems in molecules A and B have very similar conformations. The superposability of the C1–19 fragments of the two molecules was estimated by means of a best least-squares fit (15), giving a root-mean-square displacement of 0.037 Å between corresponding atoms. As shown in **Fig. 2,** the tetracyclic ring and ester linkage of molecules A and B in cholestanyl caprylate and cholesteryl myristate are also closely superposable. The rms displacements of corresponding atoms are 0.18 Å in molecule A and 0.31 Å in molecule B.

Puckering coordinates (16) for ring A in the steroid portion of cholestanyl caprylate are Q = 0.527 Å, φ = 246.2° in molecule A and Q = 0.556 Å, φ = 284.1° in molecule B. For ring B the corresponding coordinates are Q = 0.536 Å, φ = 318.8° in molecule A and Q = 0.552 Å, φ = 299.5° in molecule B. These values indicate a normal chair conformation due to the C5–C6 single bond in the tetracyclic ring system. The puckering coordinates of ring A in the steroid portion of cholesteryl myristate are Q = 0.529 Å, φ = 54.91° in molecule A and Q = 0.549 Å, φ = 42.01° in molecule B. For ring B the corresponding coordinates are Q = 0.484 Å, φ = 217.3° in molecule A and Q = 0.504 Å, φ = 213.6° in molecule B.

The caprylate chains are both almost fully extended (Figs. 1 and 2). Molecules A and B are related by a bodily movement of the caprylate chains with respect to the

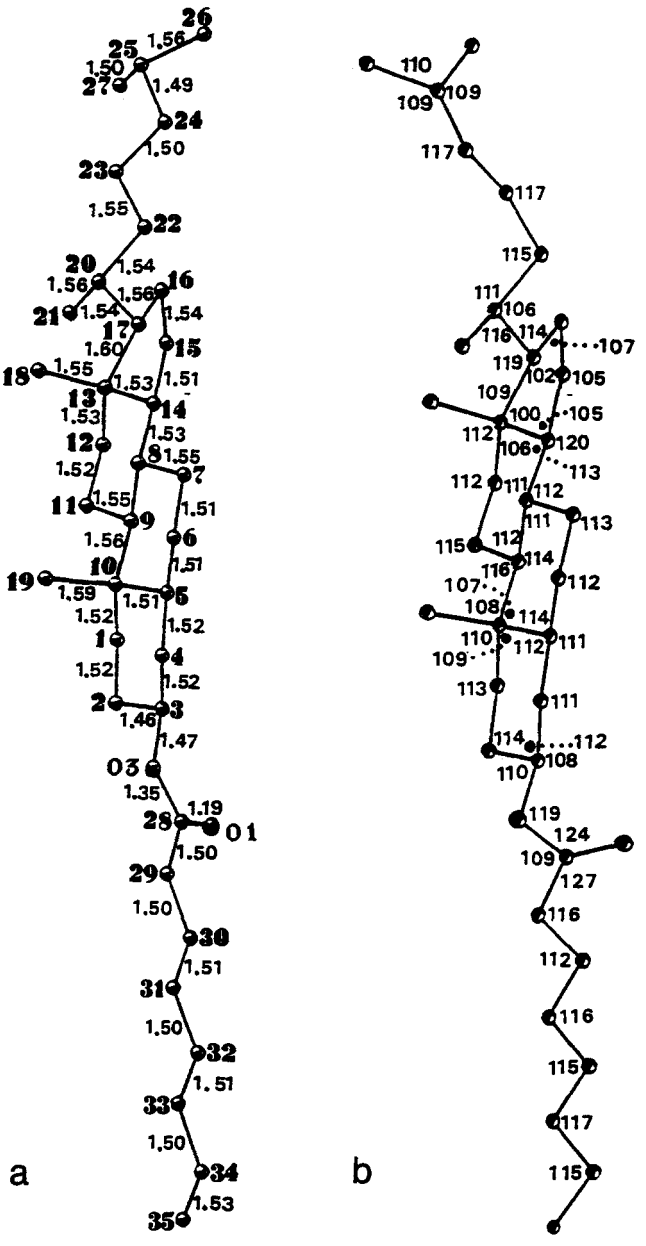

Fig. 1. *Cholestanyl caprylate with conformations observed in the crystal structure.* The tetracyclic systems of molecules A and B are shown in the same orientation. (a) Atomic nomenclature and mean bond lengths (Å) for molecules A and B. The conformation is that of molecule B. (b) The mean bond angles for molecules A and B. The conformation is that of molecule A.

[3] $R = \Sigma|\Delta|/\Sigma|Fo|$; $R_w = \{\Sigma w\Delta^2/\Sigma|Fo|2\}^{1/2}$; $S = \{\Sigma w\Delta^2/(m-n)\}^{1/2}$ where $\Delta = |Fo| - |Fc|$, m = number of reflections, n = number of parameters.

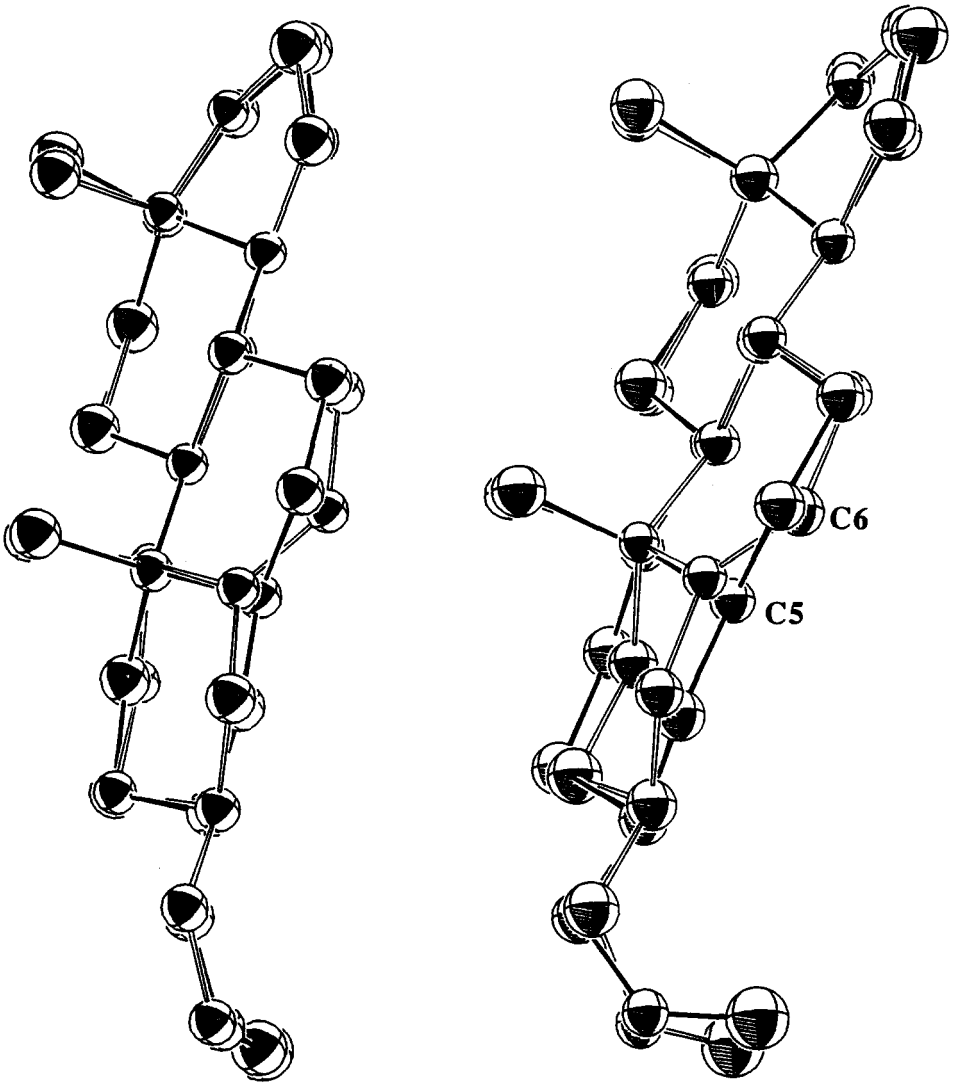

Fig. 2. Superposition of tetracyclic ring and ester linkage from the crystal structures of cholestanyl caprylate (solid bonds) and cholesteryl myristate (6). (a) Superposition of A-molecules. (b) Superposition of B-molecules.

tetracyclic steroid portion. This is evident from the difference in the torsion angle C2-C3-O3-C28 and C4-C3-O3-C28 at the ester bond which is 88°, −145°C in molecule A, and 150°, −90° in molecule B. The corresponding torsion angles in cholesteryl myristate are 87°, −154.9° in molecule A and 102°, −136° in molecule B. The carbonyl oxygen atom in molecule A is much closer to C2 than that in molecule B. In molecule A, the intramolecular O····C distance is 3.33 Å, while it is 4.10 Å in molecule B.

In molecule A, the tail group at C17 is almost fully extended (**Table 2**), but in molecule B there is a twist, giving a gauche-conformation about the C22-C23 bond. The torsion angles about C22-C23 are −178° and 68° in molecules A and B, respectively. **Table 3** lists best least-squares planes through selected atoms in each molecule. The dihedral angle between the best least-squares planes through the atoms of the tetracyclic rings and through the caprylate chain atoms is 59°C in molecule A and 61° in molecule B.

Molecular packing

The crystal structure of cholestanyl caprylate, as shown in **Fig. 3,** consists of bilayers each with thickness corresponding to $d_{001}/2$ = 43.8 Å. Within the bilayer, there is O_a orthorhombic packing of the caprylate chains, which is the same as found for the methylene subcell packing of cholesteryl myristate (6). The cholestanol ring systems of the molecules pack with each other, and caprylate chains pack with caprylate chains in an antiparallel arrangement of molecules. The efficient packing of the

TABLE 2. Torsion angles (°)

Atoms	Mol A	Mol B	Atoms	Mol A	Mol B
C10-C1-C2-C3	-49(1)	-55(1)	C2-C3-O3-C28	88(1)	150(1)
C1-C2-C3-C4	49(1)	53(1)	C4-C3-O3-C28	-145(1)	-90(1)
C2-C3-C4-C5	-52(1)	53(1)	C3-O3-C28-C29	178(1)	179(1)
C3-C4-C5-C10	56(1)	56(1)	C3-O3-C28-O1	-4(1)	4(1)
C4-C5-C10-C1	-56(1)	-56(1)	O3-C28-C29-C30	174(1)	-178(1)
C5-C10-C1-C2	52(1)	54(1)	C28-C29-C30-C31	-179(1)	-179(1)
C10-C5-C6-C7	-57(1)	-56(1)	C29-C30-C31-C32	-178(1)	180(1)
C5-C6-C7-C8	48(1)	49(1)	C30-C31-C32-C33	-179(1)	179(1)
C6-C7-C8-C9	-46(1)	-48(1)	C31-C32-C33-C34	-179(2)	178(1)
C7-C8-C9-C10	51(1)	53(1)	C32-C33-C34-C35	178(1)	-179(1)
C8-C9-C10-C5	-55(1)	-57(1)	C17-C13-C14-C15	47(1)	45(1)
C9-C10-C5-C6	57(1)	59(1)	C4-C5-C10-C9	-176(1)	-173(1)
C8-C9-C11-C12	49(1)	51(1)	C1-C10-C5-C6	177(1)	176(1)
C9-C11-C12-C13	-56(1)	-55(1)	C7-C8-C9-C11	-176(1)	-176(1)
C11-C12-C13-C14	57(1)	57(1)	C10-C9-C8-C14	179(1)	178(1)
C12-C13-C14-C8	-59(1)	-61(1)	C12-C13-C14-C15	167(1)	168(1)
C13-C14-C8-C9	57(1)	61(1)	C8-C14-C13-C17	180(1)	177(1)
C14-C8-C9-C11	-48(1)	-52(1)	C4-C5-C10-C19	66(1)	67(1)
C13-C14-C15-C16	-34(1)	-35(1)	C8-C14-C13-C18	65(1)	61(1)
C14-C15-C16-C17	7(1)	11(1)	C13-C17-C20-C21	-55(1)	-55(1)
C15-C16-C17-C13	21(1)	17(1)	C13-C17-C20-C22	-178(1)	-178(1)
C16-C17-C13-C14	-40(1)	-38(1)	C17-C20-C22-C23	-171(1)	-164(1)
C4-C5-C6-C7	176(1)	176(1)	C20-C22-C23-C24	-178(1)	68(2)
			C22-C23-C24-C25	179(1)	174(1)

molecules inside the bilayers does not extend to the C17 tails which form the outer bilayer surfaces. Thus, densities calculated for the three different strata within a bilayer are 0.75 for the tails C20-C27 (fractional z coordinates in the range $0 \leq z \geq 0.074$), 1.15 for the cholestanol ring atoms C1-C19 ($0.074 \leq z \geq 0.184$), and 1.07 $g \cdot cm^{-3}$ for the caprylate chains including ester oxygen atoms ($0.184 \leq z \geq 0.316$). Corresponding densities for cholesteryl myristate are 0.75, 1.18, and 1.02 $g \cdot cm^{-3}$.

TABLE 3. Best least-squares planes

(a) Plane constants. Values for molecule A above those for molecule B

Plane	a	b	c	d
(1)	9.725	0.074	22.978	6.108
	9.580	-0.390	26.716	12.047
(2)	4.859	6.646	9.683	6.416
	5.240	6.456	11.410	9.437
(3)	4.810	6.706	5.222	5.527
	5.300	6.418	12.076	9.664

(b) Distances (Å) of atoms from the planes

Plane (2)			Plane (3)		
	Mol A	Mol B		Mol A	Mol B
C30	0.00	0.00	O1	-0.00	-0.01
C31	0.00	0.01	O3	-0.00	-0.01
C32	-0.00	-0.01	C28	0.01	0.03
C33	-0.02	-0.02	C29	-0.00	-0.01
C34	-0.00	0.01			
C35	0.02	0.01			

The calculated planes are as follows: (1) tetracyclic ring system, atoms C1-C17; (2) caprylate chain, atoms C30-C35; (3) ester group, atoms O3, C28, O1, C29. Equations are in the form: $ax + by + cz = d$, referred to the crystal axes, with plane constants in Å.

Inside the bilayer, there is a close proximity of polar ester groups from neighboring molecules. The carbonyl bonds from molecules A and B almost overlap in stacking along the *b* direction and are approximately antiparallel. The respective intermolecular C····O distances of 3.77 and 3.46 Å represent very weak carbonyl/carbonyl interactions.

Binary system cholestanyl caprylate/cholesteryl caprylate

Because the atoms of the cholestanyl and cholesteryl ring systems are closely superposable (Fig. 2), it might be supposed that the crystal structures of the two caprylate esters would be closely related. However, this is not so. The crystal structures of the cholesteryl n-alkanoate esters are of three types, depending primarily on chain length (17). For chains C13 and longer, the structure is of bilayer type, similar to that which is presently reported for cholestanyl caprylate. For chains C9 through C12, the crystal structures contain so-called monolayers of type I, in which alkanoate chains pack together with the cholesteryl ring systems. The C8 (3), C6 (18), and several shorter chain esters (19) adopt a different monolayer structure (type II) in which the packing together of cholesteryl rings is the predominant feature. Previous studies of phase equilibria in binary systems of cholesteryl esters by Dorset (20) have been concerned with the effects of different ester chain length. For cholesteryl myristate/cholestanyl myristate in

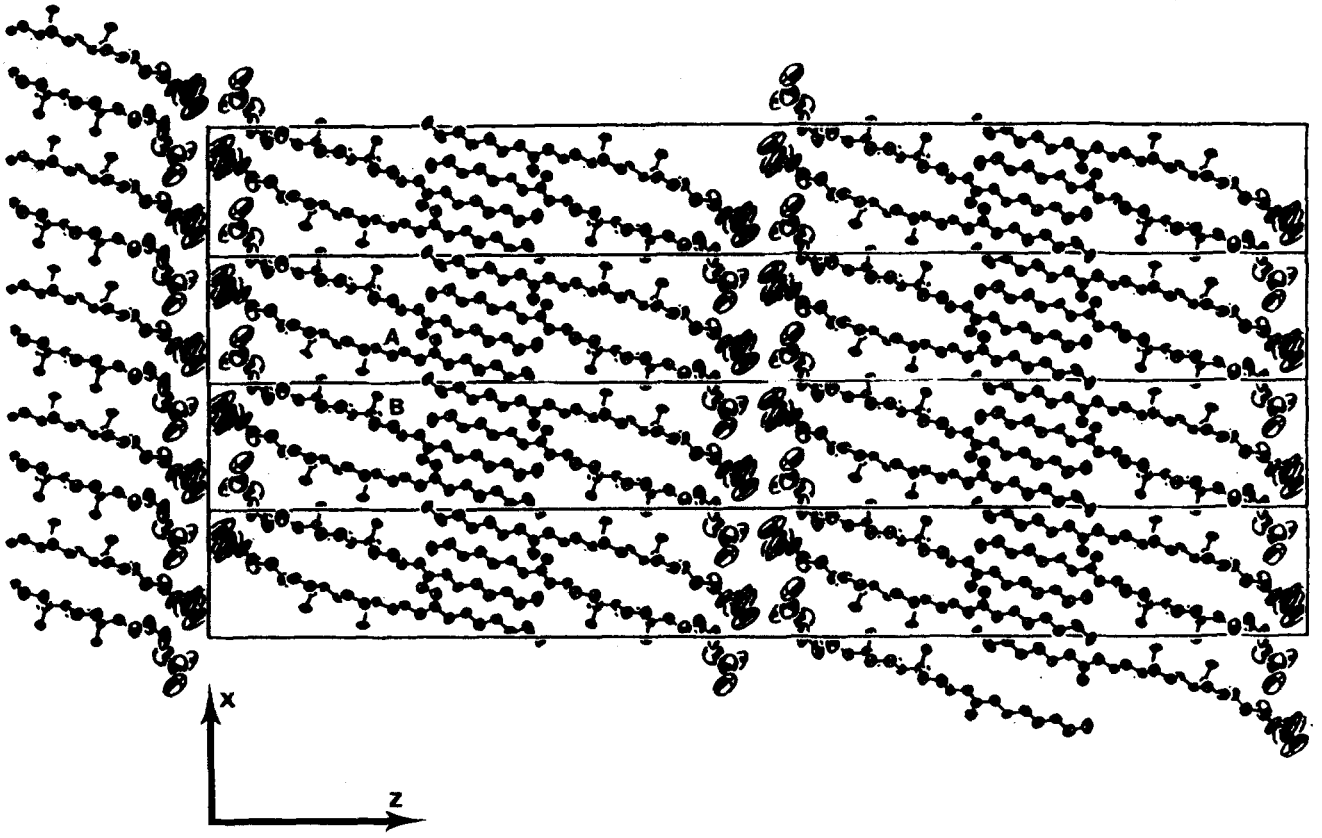

Fig. 3. The crystal structure of cholestanyl caprylate at 298 K in projection down the b axis. Each ellipsoid has 50% probability of enclosing an atom.

which both components have a bilayer crystal structure, North and Small (21) showed that solid solutions are formed at all compositions. We have carried out a study of the phase equilibria in the binary system cholestanyl caprylate/cholesteryl caprylate (**Fig. 4**) in order to determine the extent of mutual solubility when the pure components have a different crystal structure type.

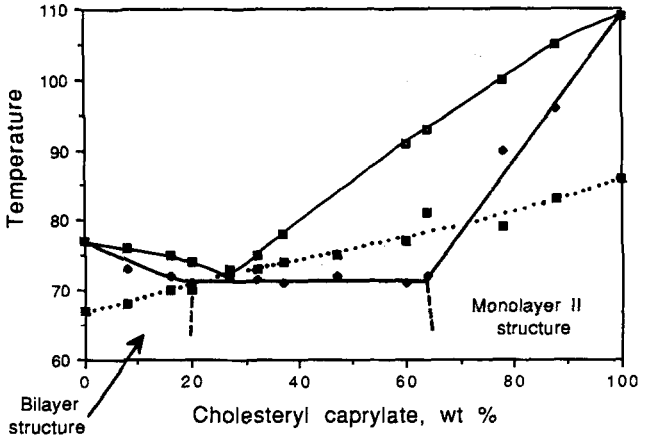

Fig. 4. Phase diagram for cholestanyl caprylate-cholesteryl caprylate. Temperatures are in °C. Data points are shown as (♦) for eutectic melting temperature; (■) for liquidus temperatures; (■) for cholesteric to isotropic liquid transition temperatures. The liquidus curves were drawn through experimental points. The latter have been fitted by least squares to a polynomial of third degree (shown as a dotted line).

Samples in the composition ranging from about 20 to 64 wt % cholesteryl caprylate exhibit a sharp melting transition at 71 ± 2°C corresponding to the melting of a eutectic mixture. The composition of the eutectic mixture is 27 wt % cholesteryl caprylate. It appears that up to about 36 wt %, the cholestanyl ester forms a solid solution in the monolayer (II) structure of the cholesteryl ester. Furthermore, the cholesteryl ester is soluble up to about 20 wt % in the bilayer structure of the cholestanyl ester. For the compositions outside the range 20 to 64 wt % of cholesteryl caprylate, X-ray powder diffraction with the samples previously used for calorimetry shows the presence of only one crystalline phase. Our analysis of powder patterns makes use of lines which do not overlap in the patterns of the individual crystal structure types. Thus the strong 004 line (d = 21.9 Å) from cholestanyl caprylate is absent in the powder pattern for the samples with 75 wt % cholesteryl caprylate and 89 wt % cholesteryl caprylate. Likewise, at compositions containing less than 20 wt % cholesteryl caprylate, X-ray powder diffraction does not show the strong 021 and 120 lines (d = 4.37, 4.33 Å) from cholesteryl caprylate.

The greater solubility of cholestanyl caprylate in the

monolayer structure was unexpected. In this crystal structure, the alkyl chains are loosely packed and cohesion seems to depend on the close packing of the steroid ring systems. A point defect, introduced by random substitution of a cholestanyl for a cholesteryl group, should cause a significant structural perturbation in the region of the steroid A and B rings as might be inferred from the superposition shown in Fig. 2. However the effect does not appear to be as disruptive as the reverse substitution of a cholesteryl for a cholestanyl group in the bilayer structure (Fig. 3).

By light microscopy, we observe the formation of a cholesteric liquid crystalline phase at all compositions. As shown in Fig. 4, this phase is metastable except for a narrow range of composition close to that of the eutectic mixture. Within this range, the enthalpy change for the transition from isotropic liquid to the cholesteric phase is 3.1 kJ/mole.

This work was supported by the National Institutes of Health, Grant HL-20350. We are grateful to Dr. R. Shiono for the use of computer programs, and also to Dr. John Ruble and Mrs. Joan Klinger for technical assistance.

Manuscript received 22 January 1991 and in revised form 1 May 1991.

REFERENCES

1. Salen, G. 1971. Cholestanol deposition in cerebrotendinous xanthomatosis. *Ann. Intern. Med.* **75:** 843–851.
2. Fumagalli, R., G. Galli, and G. Urna. 1971. Cholestanol and 26-hydroxycholesterol in normal and atherosclerotic human aorta. *Life Sci. Part II Biochem. Gen. Mol. Biol.* **10:** 25–33.
3. Craven, B. M., and N. G. Guerina. 1979. The crystal structure of cholesteryl octanoate. *Chem. Phys. Lipids.* **24:** 157–166.
4. North, B. E., G. G. Shipley, and D. M. Small. 1976. The thermal transitions and structural properties of 5α-cholestan-3β-yl esters of aliphatic acids. *Biochim. Biophys. Acta.* **424:** 376–385.
5. Sawzik, P., and B. M. Craven. 1981. Crystal data for fatty-acid esters of cholesterol and cholestanol. *J. Appl. Crystallogr.* **14:** 351–352.
6. Craven, B. M., and G. T. Detitta. 1976. Cholesteryl myristate: structures of the crystalline solid and mesophase. *J. Chem. Soc. Perkin Trans. II.* **7:** 814–822.
7. Gilmore, C. J. 1983. MITHRIL A computer program for the automatic solution of crystal structures from X-ray data. Department of Chemistry, University of Glasgow, Scotland.
8. Cromer, D. T., and J. T. Waber. 1965. Scattering factors computed from relativistic Dirac-Slater wave functions. *Acta Crystallogr.* **18:** 104–109.
9. Stewart, R. F., E. R. Davidson, and W. T. Simpson. 1965. Coherent X-ray scattering for the hydrogen atoms in the hydrogen molecule. *J. Chem. Phys.* **42:** 3175–3187.
10. Jones, T. A. 1978. A graphics model building and refinement system for macromolecules. *J. Appl. Crystallogr.* **11:** 268–272.
11. Sawzik, P., and B. M. Craven. 1982. The crystal structure of cholesteryl palmitoleate at 295 K. **B38:** 1777–1781.
12. Guerina, N. G., and B. M. Craven. 1979. The crystal structure of cholesteryl nonanoate. *J. Chem. Soc. Perkin Trans. II.* **10:** 1414–1419.
13. Craven, B. M. 1979. Pseudosymmetry in cholesterol monohydrate. *Acta Crystallogr.* **B35:** 1123–1128.
14. Sawzik, P., and B. M. Craven. 1979. The crystal structure of cholesteryl laurate. *Acta Crystallogr.* **B35:** 789–791.
15. Nyburg, S. C. 1974. Some uses of a best molecular fit routine. *Acta Crystallogr.* **B30:** 251–253.
16. Cremer, D., and J. A. Pople. 1975. A general definition of ring puckering coordinates. *J. Am. Chem. Soc.* **97:** 1354–1358.
17. Craven, B. M. 1986. Cholesterol crystal structures: adducts and esters. *In* Handbook of Lipid Research, 4. D. M. Small, editor. Plenum Press, New York. 149–182.
18. Park, Y. J., and B. M. Craven. 1981. The crystal and molecular structure of cholesteryl hexanoate at room and low temperature. *J. Korean Chem. Soc.* **3:** 131–139.
19. Seo, H. R., Y. J. Park, and B. M. Craven. 1990. Structure of cholesteryl pentyl carbonate. *J. Korean Chem. Soc.* **3:** 131–139.
20. Dorset, D. L. 1988. Co-solubility of saturated cholesteryl esters: a comparison of calculated and experimental binary phase diagrams. *Biochim. Biophys. Acta.* **963:** 88–97.
21. North, B. E., and D. M. Small. 1977. Thermal and structural properties of the cholestanyl myristate-cholesteryl myristate and cholestanyl myristate-cholesteryl oleate binary systems. *J. Phys. Chem.* **81:** 723–727.